EPJ Web of Conferences **206**, 06007 (2019) https://doi.org/10.1051/epjconf/201920606007
ISMD 2018

Convergence properties of Lévy expansions: implications for Odderon and proton structure

T. Csörgő[1,2,3,*] *R.* Pasechnik[4,**] and *A.* Ster[1,***]

[1]MTA Wigner FK, H-1525 Budapest 114, P.O.Box 49, Hungary
[2]EKE KRC, H-3200 Gyöngyös, Mátrai út 35, Hungary
[3]CERN, CH - 1211 Geneva 23, Switzerland
[4]Department of Astronomy and Theoretical Physics, Sölvegatan 14 A, SE - 223 62 Lund, Sweden

Abstract. We detail here the convergence properties of a new model-independent imaging method, the Lévy expansion, that seems to play an important role in the analysis of the differential cross section of elastic hadron-hadron scattering. We demonstrate, how our earlier results concerning the Odderon effects in the differential cross-section of elastic proton-proton and proton-antiproton scattering as well as those related to apparent sub-structures inside the protons were obtained in a convergent and stable manner.

1 Introduction

The model-independent Lévy imaging technique [1–3] has recently become a useful, simple and unambiguous tool for extracting the physics information from the elastic hadron-hadron scattering data in a statistically acceptable manner. The power of this technique has been first demonstrated in our earlier analysis of the most recent data sets from the total, elastic and differential cross-section measurements in elastic pp collisions $\sqrt{s} = 13$ TeV performed by the TOTEM Collaboration at the Large Hadron Collider (LHC) (for a few most recent TOTEM publications, see Refs. [4–7]). These TOTEM results, and in particular the comparison of the differential cross-section of elastic proton-proton scattering at $\sqrt{s} = 2.76$ TeV with D0 results on elastic proton-antiproton scattering at 1.96 TeV [8] indicate several Odderon effects, as discussed recently in Refs. [1, 7]

In particular, indirect signatures of the Odderon exchange in differential elastic pp and $p\bar{p}$ cross-sections have been identified by using the Lévy imaging technique, also known as the model-independent Lévy expansion method. Another important implication of this technique is that it enables to probe the internal structure of the proton by identifying its smaller substructures imprinted in the behaviour of the t-dependent elastic slope $B(t)$. In particular, the proton substructures of two distinct sizes in the low (a few tens of GeV) and high (a few TeV) energy regimes, respectively, have been found and discussed in Refs. [1–3]. A remarkable feature of the Lévy expansion of the elastic amplitude is that the diffractive cone is described fairly well by the Lévy-stable (or stretched exponential) distribution in terms of two free parameters only, the Lévy scale parameter R characterising the length-scale of the

*e-mail: tcsorgo@cern.ch
**e-mail: Roman.Pasechnik@thep.lu.se
***e-mail: Ster.Andras@wigner.mta.hu

scattered systems, and the exponent $\alpha = \alpha_L/2$. One of the conventions of elastic scattering is to parameterize the diffractive cone with an exponential behaviour, corresponding to $\alpha = 1$, i.e. to a Gaussian scattering amplitude in the impact parameter space. The exponent $\alpha_L = 2\alpha$ is known as the Lévy index of stability providing a small but significant deviation of the cone shape from the classically expected Gaussian shape. A detailed presentation of this sophisticated new imaging technique is detailed in Ref. [1], while for a brief summary of the main results, see Refs. [2, 3].

Given a power of the Lévy imaging technique operating with very few initial assumption for description of a large amount of data, a natural question arises about the stability and convergence of the associated Lévy series that are used for mapping the elastic amplitude with this method. In this contribution, we attempt to give a short description of the main results of the method, as well as demonstrate its convergence properties for a large variety of data sets at different scattering energies. The main results were summarized recently in two short contributions [2, 3], however the convergence properties of this model-independent Lévy expansion method were not yet detailed in the literature before.

2 Model-independent Lévy expansion of the scattering amplitude

In order to study systematically the deviations of a given data set on the elastic cross section $d\sigma/dt$, differential in four-momentum transfer $t = (p_1 - p_3)^2 < 0$, from an approximate Lévy-stable shape apparent at larger t beyond the diffractive cone, we adopt the Lévy series expansion for the elastic amplitude $T_{\rm el}(\Delta)$, $\Delta = \sqrt{|t|}$, represented in terms of a complete orthonormal set of Lévy polynomials (with complex coefficients) and a Lévy weight function $w(z|\alpha) = \exp(-z^\alpha)$ [1, 2]. While the Lévy polynomials exhibit an oscillatory behaviour in dimensionless scaling variable $z = |t|R^2$, the differential cross-section of elastic scattering is proportional to a hit distribution which is, by construction, a positively-definite function of t, i.e.

$$\frac{d\sigma}{dt} = \frac{1}{4\pi}|T_{\rm el}(\Delta)|^2\,, \quad T_{\rm el}(\Delta) \;=\; i\sqrt{4\,\pi\,A\,w(z|\alpha)}\left[1 + ib_0 + \sum_{i=1}^{\infty} c_i l_i(z|\alpha)\right], \tag{1}$$

where $c_j = a_j + ib_j$ are the complex coefficients of the Levy expansion ($j = 0, 1, ...,$) and $a_0 = 1$ fixed so that the overall normalization can be absorbed into the coefficient A. This simple expansion form indicates three underlying physical assumptions, with further details explained below.

1. The leading order behaviour corresponds to a nearly exponential (in other words, a non-exponential) distribution. This leading order behaviour is $\frac{d\sigma}{dt} = A\exp\left[-(R^2|t|)^\alpha\right]$, which is consistent with the TOTEM observation of a non-exponential low-$|t|$ behaviour of the differential cross-section of elastic pp scattering at $\sqrt{s} = 8$ TeV [9]. In the limit of $\alpha \to 1$, the exponential cone behaviour is recovered, with $\lim_{\alpha\to 1}\frac{d\sigma}{dt} = A\exp\left[-B|t|\right]$ with $B = R^2$.

2. The leading order scattering amplitude is assumed to be imaginary, with vanishing real part, corresponding to $b_0 = 0$ and to all the c_j expansion coefficients vanish for $j \geq 1$. Such an assumption can be relaxed by assuming that b_0 can be different from zero, but so far all the fits that we have performed, we have found b_0 to be consistent within errors with zero, so we have fixed this possible expansion parameter to zero, accordingly. The possibility of relaxing b_0 to be different from zero is investigated in Fig. 1 and it is briefly discussed there in the context of the $\sqrt{s} = 13$ TeV elastic pp scattering data.

3. For predominantly imaginary scattering amplitudes with $b_0 = 0$, the existence of a non-vanishing real to imaginary ratio $\rho(t)$, in particular, $\rho_0 = \rho(t = 0)$, is mapped one-to-one to the existence of a diffractive interference structure, i.e. a diffractive minimum in elastic scattering cross section. Given that for $t \neq 0$ the Levy expansion is an analytic function, and that at the first diffractive minimum the imaginary part is expected to vanish, the phase of the scattering amplitude can be uniquely determined with the Lévy expansion method up to an overall sign, that can be fixed from measurements at the Coulomb-nuclear interference region. This implies that the ρ_0 parameter can be determined from the Lévy expansions if the fit range includes a diffractive minimum.

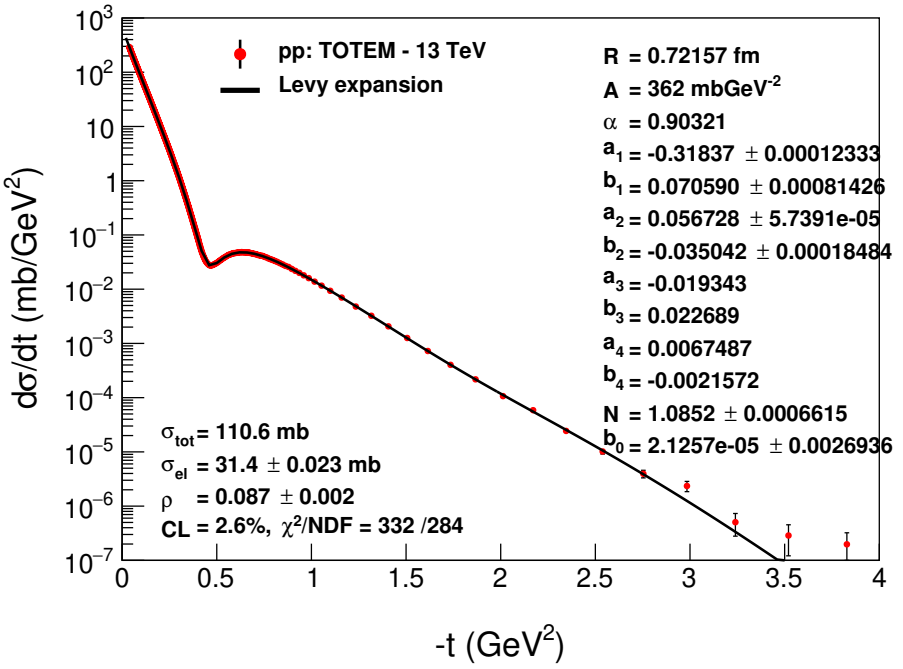

Figure 1. Fourth order Levy expansion to $\sqrt{s} = 13$ TeV pp elastic scattering data using Eq. (1) with a b_0 as a free parameter. The comparision to the TOTEM data from Ref. [6] resulted in a statistically acceptable description within quadratically added statistical and systematic errors. The fit parameter b_0 was within errors found to be zero, hence it was fixed to zero in the subsequent analysis.

The set of orthonormal polynomials are denoted above by $\left\{l_j(z|\alpha)\right\}_{j=0}^{\infty}$, while the set of orthogonal, but unnormalized Lévy polynomials are denoted by $\left\{L_j(z|\alpha)\right\}_{j=0}^{\infty}$. These unnormalized Lévy polynomials were introduced in Refs. [10, 11], to analyze nearly Lévy shaped Bose-Einstein correlations in two-particle Bose-Einstein correlations or particle interferometry. Their orthogonality is defined with respect to the weight function $w(z|\alpha) = \exp(-|z|^{\alpha})$ where the dimensionless variable $z = |t|R^2$. The weight function acts simultaneously as the leading order approximate form of the measured distribution, and at the same time also as a measure in an abstract Hilbert space, where the convergence properties of the Lévy series

can be investigated, following the general ideas proposed in Ref. [12]. Thus, this expansion method allows to keep the number of expansion coefficients at the minimal necessary level.

The orthonormality of the Lévy polynomials $l_n(z\,|\,\alpha)$ is expressed as

$$\int_0^\infty dz \exp(-z^\alpha)\, l_n(z\,|\,\alpha)\, l_m(z\,|\,\alpha) \quad = \quad \delta_{n,m}\,. \tag{2}$$

These orthonormalized polynomials $l_j(z\,|\alpha)$ are proportional to the orthogonal – but unnormalized — Lévy polynomials, $L_j(z\,|\,\alpha)$,

$$l_j(z\,|\,\alpha) \quad = \quad D_j^{-\frac{1}{2}}(\alpha)\, D_{j+1}^{-\frac{1}{2}}(\alpha)\, L_j(z\,|\,\alpha)\,, \qquad \text{for } j \geq 0, \tag{3}$$

which in turn are given by a Gram-Schmidt orthogonalization procedure as

$$L_0(z\,|\,\alpha) \quad = \quad 1, \tag{4}$$

$$L_1(z\,|\,\alpha) \quad = \quad \det\begin{pmatrix} \mu_{0,\alpha} & \mu_{1,\alpha} \\ 1 & z \end{pmatrix}, \tag{5}$$

$$L_2(z\,|\,\alpha) \quad = \quad \det\begin{pmatrix} \mu_{0,\alpha} & \mu_{1,\alpha} & \mu_{2,\alpha} \\ \mu_{1,\alpha} & \mu_{2,\alpha} & \mu_{3,\alpha} \\ 1 & z & z^2 \end{pmatrix}, \quad \ldots \text{ etc}\,. \tag{6}$$

introduced previously in Ref. [10]. The Gram-determinants of order j, $D_j \equiv D_j(\alpha)$ defined as

$$D_0(\alpha) \quad = \quad 1, \tag{7}$$

$$D_1(\alpha) \quad = \quad \mu_{0,\alpha}, \tag{8}$$

$$D_2(\alpha) \quad = \quad \det\begin{pmatrix} \mu_{0,\alpha} & \mu_{1,\alpha} \\ \mu_{1,\alpha} & \mu_{2,\alpha} \end{pmatrix}, \tag{9}$$

$$D_3(\alpha) \quad = \quad \det\begin{pmatrix} \mu_{0,\alpha} & \mu_{1,\alpha} & \mu_{2,\alpha} \\ \mu_{1,\alpha} & \mu_{2,\alpha} & \mu_{3,\alpha} \\ \mu_{2,\alpha} & \mu_{3,\alpha} & \mu_{4,\alpha} \end{pmatrix}, \quad \ldots \text{ etc.} \tag{10}$$

In the above expressions,

$$\mu_{n,\alpha} = \int_0^\infty dz\, z^n \exp(-z^\alpha) = \frac{1}{\alpha}\,\Gamma\left(\frac{n+1}{\alpha}\right), \quad \Gamma(x) = \int_0^\infty dz\, z^{x-1} e^{-z}\,, \tag{11}$$

where $\Gamma(x)$ the Euler's gamma function.

3 Observables

Observables can be calculated from Eq. (1). In what follows, we present the results for the fixed $b_0 = 0$.

The total cross-section is obtained, using the optical theorem, as follows

$$\sigma_{\rm tot} \equiv 2\,{\rm Im}\, T_{\rm el}(\Delta = 0) \;= 2\,\sqrt{4\pi A}\left(1 + \sum_{i=1}^{\infty} a_i l_i(0|\alpha)\right). \tag{12}$$

The elastic cross-section, $\sigma_{\rm el}$ can be obtained using the orthonormality, Eq. (2) as

$$\sigma_{\rm el} \;=\; \int_{-t=0}^{\infty} dt \frac{d\sigma}{dt} \;=\; \frac{A}{R^2}\left[\frac{1}{\alpha}\Gamma\left(\frac{1}{\alpha}\right) + \sum_{i=1}^{\infty}(a_i^2 + b_i^2)\right]. \tag{13}$$

The following t-dependent functions have also been analyzed:

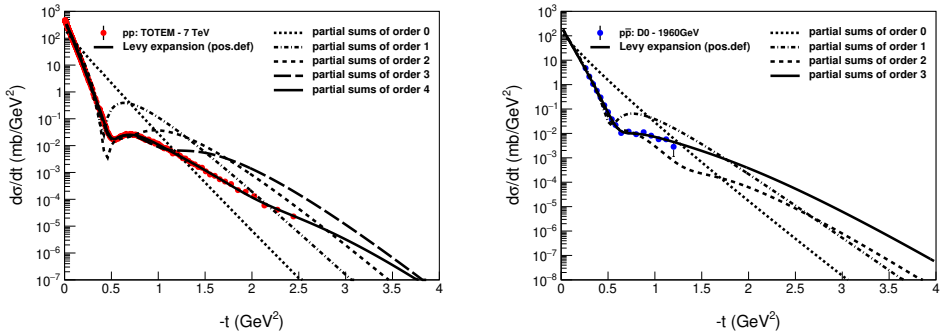

Figure 2. Partial sums from leading order to fourth order Levy expansion, as compared to the TOTEM data from Ref. [13] at $\sqrt{s} = 7$ TeV pp (left) and to D0 data from Ref. [8] on $p\overline{p}$ elastic scattering at $\sqrt{s} = 1.96$ TeV (right) elastic scattering.

- The four-momentum transfer dependent elastic slope $B(t)$, defined as

$$B(t) = \frac{d}{dt}\left(\ln\frac{d\sigma}{dt}\right). \tag{14}$$

- The four-momentum dependent $\rho(t)$, defined as the ratio of the real to imaginary parts of $T_{\rm el}$

$$\rho(t) \equiv \frac{\mathrm{Re}\, T_{\rm el}(t)}{\mathrm{Im}\, T_{\rm el}(t)} = -\left.\frac{\sum_{i=1}^{\infty} b_i I_i(z|\alpha)}{1+\sum_{i=1}^{\infty} a_i I_i(z|\alpha)}\right|_{z=tR^2}. \tag{15}$$

  The value of $\rho(t)$ at $t = 0$ can be measured in the Coulomb-nuclear interference region and in this work we refer to this value as $\rho_0 = \rho(t = 0)$.

- The first definition for the nuclear phase $\phi_1(t)$, that can be introduced as

$$T_{\rm el}(t) = |T_{\rm el}(t)| \exp\left[i\phi_1(t)\right]. \tag{16}$$

  An alternative definition was used recently by the TOTEM collaboration, corresponding to the principal value of the nuclear phase, that reads as

$$\phi_2(t) = \frac{\pi}{2} - \arctan\rho(t). \tag{17}$$

  If the nuclear phase $\phi_1(t)$ satisfies $0 \le \phi_1(t) \le \pi$, then the above two definitions are equivalent. However, for complex arguments, $\arctan(z)$ has branch cut discontinuities on the complex plane hence in general the two definitions $\phi_1(t)$ and $\phi_2(t)$ are inequivalent, as detailed recently in Ref. [1]. In the present work we plot the principal value of the nuclear phase, that corresponds to the definition with Eq. (17), which by definition satisfies $0 \le \phi_2(t) \le \pi$.

- We shall also study the convergence properties of the shadow profile function,

$$P(b) \equiv 1 - \left|e^{-\Omega(b)}\right|^2 = [2 - \mathrm{Im}\, t_{\rm el}(b)]\mathrm{Im}\, t_{\rm el}(b) - [\mathrm{Re}\, t_{\rm el}(b)]^2, \tag{18}$$

  where $\Omega(b)$ is the complex-valued opacity function. These functions can be represented in terms of the impact-parameter dependent elastic amplitude $t_{\rm el}(b)$, see for example Ref. [1]:

$$t_{\rm el}(b) = \int \frac{d^2\Delta}{(2\pi)^2}\, e^{-i\boldsymbol{\Delta b}}\, T_{\rm el}(\Delta) = i\left[1 - e^{-\Omega(b)}\right], \quad \Delta \equiv |\boldsymbol{\Delta}|, \quad b \equiv |\boldsymbol{b}|. \tag{19}$$

4 Convergence properties

The Lévy series (1) enables one to precisely and model-independently characterise the t-dependence of the elastic cross-section $\frac{d\sigma}{dt}$ not only in the diffractive cone, but also significantly away from it, namely, in a vicinity of the diffractive minimum as well as beyond it in the large t regime (diffractive tail). This is achieved by a fit of Eq. (1) to the existing data controlling the fit quality and the convergence of the Lévy ansatz to the data points in each particular region of 4-momentum transfers.

We adopted the following procedure: a fourth order Lévy polynomial fit was performed to the measured $\frac{d\sigma}{dt}$ data for elastic pp scattering. The expansion coefficients (a_i, b_i) are determined for $i = 1, ..., i_{\max} = 4$. On the subsequent plots, the contributions are summed only up to a given order $j \leq i_{\max}$. Thus a procedure not unlike to a Taylor series expansion is defined and the inclusion of each subsequent order enables us to see how the series converges to the measurements on a more and more extended domain. As described in Ref. [1], good quality fits of elastic pp scatterings were achieved for almost all of the published data sets, using $i_{\max} = 4$. To fit the $p\bar{p}$ datasets, that were measured in a more limited t-range and with reduced statistics, third order Levy expansions with $i_{\max} = 3$ were sufficient.

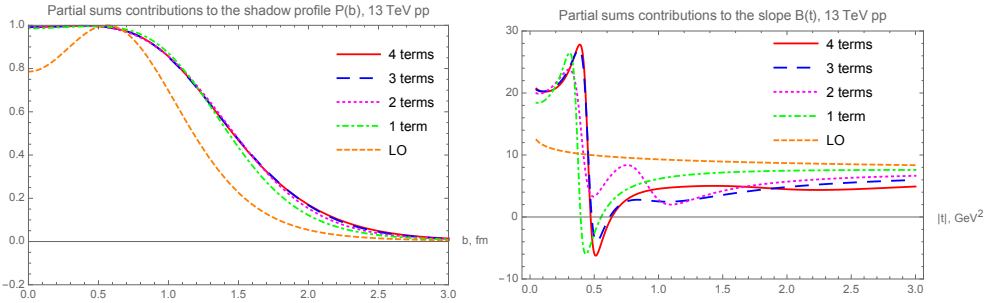

Figure 3. The shadow profile (left) and the elastic slope (right) with partial sums from leading order to fourth order Levy expansion, fitted to the TOTEM data at $\sqrt{s} = 13$ TeV pp elastic scattering.

As we demonstrate below, these fits converge rather fast to the data when increasing the order of the Lévy expansion from zeroth to the fourth order.

As an example of the convergence property, in Fig. 2, we illustrate partial sums contributions to the Lévy series (1) for the differential elastic cross-section against the TOTEM 7 TeV (left) and D0 1.96 TeV (right) data sets. As Figure 2 indicates, the zeroth order term fixes the total cross-section, i. e. the contribution at $t = 0$ only, it apparently insufficient even at small t to approximate the shape of the distribution. The first order Lévy expansions is required to describe $B(t = 0)$ and the beginining of the diffractive cone. Although the first order contribution exhibits a structure with a diffractive dip, the position and the size of the dip is not yet picked up correctly. The second order partial sum is needed for getting the position of the diffractive minimum correctly, while the third order term fixes the position and the magnitude of the diffractive maximum. The forth order terms are necessary to describe the data also well beyond the diffractive minimum and maximum.

While at zeroth order the real part of the elastic amplitude is found to be vanishing in our current approach, it may get (re)generated starting from the first order partial sums, and appears to be necessarily small. Remarkably, the considered quality fits shown for example in Fig. 1 for the 13 TeV elastic pp scattering data of TOTEM enable us to reproduce the measured real-to-imaginary parts ratio $\rho(t)$ at $t = 0$ with an excellent precision.

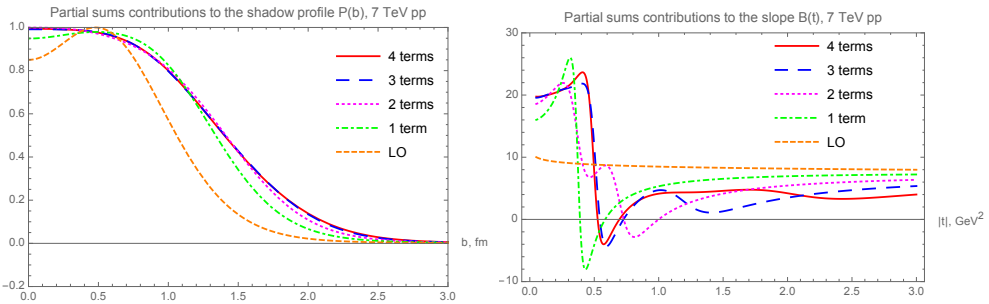

Figure 4. The shadow profile (left) and the elastic slope (right) with partial sums from leading order to fourth order Levy expansion, fitted to the TOTEM data at $\sqrt{s} = 7$ TeV pp elastic scattering.

In Figs. 3, 4 and 5 we show the convergence properties of the shadow profile (left panels) and the elastic slope (right panels) for Lévy fits of the TOTEM data at 13 TeV, 7 TeV (pp collisions) and D0 data at 1.96 TeV ($p\bar{p}$ collisions) at different consecutive orders as previously illustrated in Fig. 2, respectively.

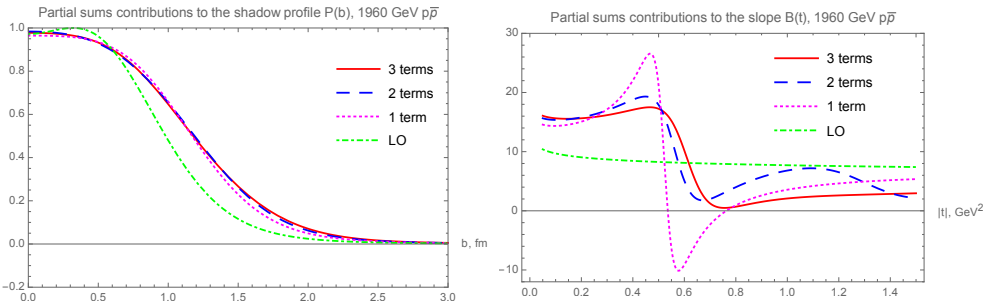

Figure 5. The shadow profile (left) and the elastic slope (right) with partial sums from leading order to third order Levy expansion fitted to the D0 data at $\sqrt{s} = 1.96$ TeV $p\bar{p}$ elastic scattering.

The convergence of partial sums contributions to the shadow profile turns out to be faster than that for the elastic slope. Namely, already starting from the second Lévy order the result for $P(b)$ remains fairly stable at large b for all the considered data sets, but higher order terms are needed for a precise result at small values of b. For pp collisions TOTEM data at 13 and 7 TeV, the behavior of the elastic slope stabilizes in a vicinity of the diffractive dip/bump structure only at third Lévy order, in consistency with the observations made from Fig. 2. So, for all TOTEM data sets the minimal preferred order enabling to extend the data description significantly beyond the dip/bump structure is the forth. Due to a lack of data in the large-t region for $p\bar{p}$ collisions at 1.96 TeV, we limit ourselves to the third order that provides the results for $B(t)$ sufficiently stable in the "shoulder" region.

Finally, in Fig. 6 we demonstrate the corresponding convergence property of $\phi_2(t)$, the principal value of the nuclear phase for $\sqrt{s} = 13$ TeV pp elastic scattering. We observe that there is no significant difference between the third- and the forth-order Lévy expansion results indicating a good stability property of this function in the range of the diffractive minimum, where $\phi_2(t_{\rm dip}) = \pi$.

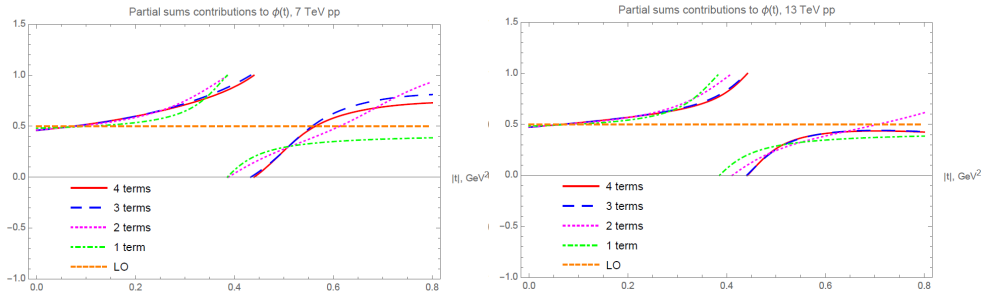

Figure 6. The principal value of the nuclear phase $\phi_2(t)$ with the contributions of the partial sums from the leading order to fourth order Levy expansion, as fitted to the TOTEM pp elastic scattering data at $\sqrt{s} = 7$ TeV (left panel) and at $\sqrt{s} = 13$ TeV (right panel), respectively. Note that stability of the point where $\phi_2(t) = \pi$ for increasing order of the expansion, and for changing the energy of the collision.

5 Odderon

The concept of Odderon exchange corresponds to a crossing-odd term in the pp elastic scattering amplitude. This concept was introduced by Lukaszuk and Nicolescu in 1973 [14].

The recent TOTEM results [4, 5] generated a burst of high level and intense theoretical debate about the correct interpretation of these data, see ref. [17]- ref [29]. All possible extreme views were present among these first interpretative papers, including claims for a maximal Odderon effect [25] and claims of lack of any significant Odderon effects, refs. [22, 29]. A review of recent theoretical developments on possible Odderon effects is given in refs. [30, 31].

At sufficiently high energies, the relative contributions from secondary Regge trajectories is suppressed, as they decay as a negative powers of the colliding energy $\sqrt{s}$. The vanishing nature of these Reggeon contributions offers a direct way of extracting the Odderon as well as the Pomeron contributions, $T^O_{el}(s,t)$ and $T^P_{el}(s,t)$, respectively, from elastic scattering data at sufficiently high colliding energies. Thus Odderon effects can be detected clearly with measurements in the TeV energy range [15, 16].

In Ref. [32], the authors also argued that the LHC energy scale is already sufficiently large to suppress the Reggeon contributions, and they presented the (s,t) dependent contributions of Odderon exchange to the differential and total cross-sections at LHC energies. That analysis relied on a model-dependent, phenomenological extension of the Phillips-Barger model [33], that focused on fitting the dip region of elastic proton-proton scattering, but did not analyze in detail the tails and the cone region. The fitted model parameters of proton-proton and proton-antiproton reactions were extrapolated to exactly the same energies, and the results were recently confirmed and extended in Ref. [34]. Similarly, Ref. [24] also argued that the currently highest LHC energy of $\sqrt{s} = 13$ TeV is sufficiently high to see various Odderon contributions. In particular, the Pomeron and the Odderon contributions can be extracted from the forward scattering amplitudes at sufficiently high energies as discussed, for example, in refs. [1, 32]. Elastic proton -proton and proton-antiproton scattering data were not measured at the same energy in the TeV region so far. However, we have identified two robust-looking features of the already performed measurements, that provided not only an Odderon signal, but they also clearly indicated the existence of two different sizes for some sub-structures inside the protons, as imaged by elastic proton-proton scattering.

In particular, we found that clear, but indirect signals of Odderon effects are present in the difference between the t-dependent nuclear slopes of elastic proton-proton and proton-antiproton scattering [1, 3]. Our results for the existence of a well-defined and negative minimum of the $B(t)$ functions for pp reactions and a lack of significantly negative values of $B(t)$ in $p\overline{p}$ reactions at the TeV region has recently been confirmed using the maximal Odderon model of Martynov and Nicolescu in ref. [39]. From the experimental point of view, $B(t)$ is straightforward to measure and can be used for an experimental search for Odderon effects independently of Lévy expansion and imaging results.

In addition, we have also identified a clear difference between the principal values of the nuclear phase, $\phi_2(t)$ of proton-proton and proton-antiproton collisions in the TeV energy range [1, 3]. However, the t-dependence of the nuclear phase is rather difficult, close to impossible to access experimentally, in particular independently of Lévy imaging methods.

Both of these Odderon effects are obtained with a convergent series expansion, and are stable for higher order Lévy expansion coefficients, as indicated on the right panels of Figs. 3, 4 and 5 in case of the nuclear slope $B(t)$ and on Fig. 6 in case of the principal value of the nuclear phase $\phi_2(t)$.

6 Summary and conclusions

Our analysis in refs. [1–3] has been primarily motivated by the search for Odderon effects. We have identified two independent Odderon effects in TOTEM differential cross-section measurements. The comparision of $B(t)$ for pp and $p\overline{p}$ reactions at exactly the same $\sqrt{s}$ in the TeV region is one of the most promising channel for the experimental observation of Odderon effects.

One of the most obvious but nevertheless striking feature of the elastic pp scattering at TeV energies is that the differential cross-section has a unique, single minimum. In multiple diffractive scattering theory, single diffractive minimum may appear in symmetric collisions of composite objects if and only if the colliding systems have two internal substructures [35]. This suggests that the quark-diquark picture of elastic proton-proton collisions, where a diquark that acts as a single unit in elastic scattering even at the LHC energies, formulated in terms of the real extended Bialas-Bzdak model of elastic proton-proton scattering [40, 41], may indeed capture correctly some of the most fundamental properties of elastic proton-proton collisions at the LHC energies.

One of our most surprising result was a clear-cut evidence for two different sub-structures inside the protons, as detailed in Ref. [1]. We determined the significance of these substructure effects and estimated the sizes of these sub-structures and their contributions to the total and elastic proton-proton cross-section in ref. [2].

Acknowledgments

We would like to thank S. Giani, G. Gustafson, V. Khoze, F. Nemes, B. Nicolescu and K. Österberg for inspiring and clarifying discussions. T. Cs. expresses his gratitude to the Organizers of ISMD 2018 for the opportunity to present these results, for partial support and for an outstanding, inspiring and useful meeting. T. Cs. was partially supported by the Hungarian NKIFH grants FK-123842 and FK-123959 and the EFOP-3.6.1-16-2016-00001 grants (Hungary). R.P. was partially supported by the Swedish Research Council grants, contract numbers 621-2013-4287 and 2016-05996, CONICYT grant MEC80170112, and by the Ministry of Education, Youth and Sports of the Czech Republic project LT17018. This research was partially supported by the THOR project, COST Action CA15213 of the European Union.

References

[1] T. Csörgő, R. Pasechnik and A. Ster, Eur. Phys. J. C **79**, no. 1, 62 (2019)
[2] T. Csörgő, R. Pasechnik and A. Ster, arXiv:1811.08913 [hep-ph].
[3] T. Csörgő, R. Pasechnik and A. Ster, arXiv:1902.00109 [hep-ph].
[4] G. Antchev *et al.* [TOTEM Collaboration], Eur. Phys. J. C **79**, no. 2, 103 (2019)
[5] G. Antchev *et al.* [TOTEM Collaboration], arXiv:1812.04732 [hep-ex].
[6] G. Antchev *et al.* [TOTEM Collaboration], arXiv:1812.08283 [hep-ex].
[7] G. Antchev *et al.* [TOTEM Collaboration], arXiv:1812.08610 [hep-ex].
[8] V. M. Abazov *et al.* [D0 Collaboration], Phys. Rev. D **86**, 012009 (2012)
[9] G. Antchev *et al.* [TOTEM Collaboration], Nucl. Phys. B **899**, 527 (2015)
[10] M. B. De Kock, H. C. Eggers and T. Csörgő, PoS WPCF **2011**, 033 (2011)
[11] T. Novák, T. Csörgő, H. C. Eggers & M. De Kock, Acta Phys. Pol. Supp. **9**, 289 (2016)
[12] T. Csörgő and S. Hegyi, Phys. Lett. B **489**, 15 (2000)
[13] G. Antchev *et al.* [TOTEM Collaboration], EPL **101**, no. 2, 21002 (2013).
[14] L. Lukaszuk and B. Nicolescu, Lett. Nuovo Cim. **8**, 405 (1973).
[15] R. Avila, P. Gauron and B. Nicolescu, Eur. Phys. J. C **49**, 581 (2007)
[16] E. Martynov and B. Nicolescu, Phys. Lett. B **778**, 414 (2018)
[17] A. P. Samokhin and V. A. Petrov, Nucl. Phys. A **974**, 45 (2018)
[18] V. A. Khoze, A. D. Martin and M. G. Ryskin, Phys. Rev. D **97**, no. 3, 034019 (2018)
[19] V. A. Petrov, Eur. Phys. J. C **78**, no. 3, 221 (2018) Erratum: [Eur. Phys. J. C **78**, no. 5, 414 (2018)]
[20] V. A. Khoze, A. D. Martin and M. G. Ryskin, Phys. Lett. B **780**, 352 (2018)
[21] V. P. Gonçalves and B. D. Moreira, Phys. Rev. D **97**, no. 9, 094009 (2018)
[22] Y. M. Shabelski and A. G. Shuvaev, Eur. Phys. J. C **78**, no. 6, 497 (2018)
[23] M. Broilo, E. G. S. Luna and M. J. Menon, Phys. Lett. B **781**, 616 (2018)
[24] P. Lebiedowicz, O. Nachtmann and A. Szczurek, Phys. Rev. D **98**, 014001 (2018)
[25] E. Martynov and B. Nicolescu, Phys. Lett. B **786**, 207 (2018)
[26] S. M. Troshin and N. E. Tyurin, Mod. Phys. Lett. A **33**, no. 35, 1850206 (2018)
[27] I. M. Dremin, Universe **4**, no. 5, 65 (2018).
[28] W. Broniowski, L. Jenkovszky, E. Ruiz Arriola and I. Szanyi, Phys. Rev. D **98**, (7), 074012 (2018)
[29] V. A. Khoze, A. D. Martin and M. G. Ryskin, Phys. Lett. B **784**, 192 (2018)
[30] E. Martynov and B. Nicolescu, arXiv:1811.07635 [hep-ph].
[31] E. Martynov and B. Nicolescu, arXiv:1810.08930 [hep-ph].
[32] A. Ster, L. Jenkovszky and T. Csörgő, Phys. Rev. D **91**, no. 7, 074018 (2015)
[33] R. J. N. Phillips and V. D. Barger, Phys. Lett. **46B**, 412 (1973).
[34] V. P. Gonçalves and P. V. R. G. Silva, arXiv:1811.12250 [hep-ph].
[35] W. Czyz and L. C. Maximon, Annals Phys. **52**, 59 (1969).
[36] G. Antchev *et al.* [TOTEM Collaboration], Eur. Phys. J. C **76**, no. 12, 661 (2016)
[37] F. J. Nemes, PoS DIS **2017**, 059 (2018).
[38] T. Csörgő [TOTEM Collaboration], EPJ Web Conf. **120**, 02004 (2016)
[39] E. Martynov and B. Nicolescu, arXiv:1808.08580 [hep-ph].
[40] A. Bialas and A. Bzdak, Acta Phys. Polon. B **38**, 159 (2007)
[41] F. Nemes, T. Csörgő and M. Csanád, Int. J. Mod. Phys. A **30**, no. 14, 1550076 (2015)